Possible impact of an unrestrained increase of ozone depleting substances on Northern Hemisphere climate

Judith Perlwitz[1,2], Ryan L. Fogt[2], Paul A. Newman[3], Luke D. Oman[4], Steven Pawson[5]

[1]Cooperative Institute for Research in Environmental Sciences, University of Colorado, Boulder, Colorado, USA

[2]NOAA Earth System Research Laboratory, Physical Sciences Division, Boulder, Colorado, USA

[3]Atmospheric Chemistry and Dynamics Branch, NASA Goddard Space Flight Center, Greenbelt, Maryland, USA

[4]Department of Earth and Planetary Sciences, Johns Hopkins University, Baltimore, Maryland, USA

[5]Global Modeling and Assimilation Office, NASA Goddard Space Flight Center, Greenbelt, Maryland, USA

Abstract

The Northern Hemisphere (NH) climate response to uncontrolled emissions of ozone-depleting substances (ODSs) at an annual increase of 3% (so called World Avoided, WA by the Montreal Protocol) is investigated. To determine possible tropospheric climate impacts of the Montreal Protocol, we analyze a WA simulation and an ensemble of reference simulations for the period of 2001 to 2049 from a coupled chemistry climate model. We found a significant shift of the Northern Hemisphere Annular Mode towards its positive phase during the late spring to fall. We show that greenhouse gas induced warming over the NH continents would be amplified by up to 100 % and the storm tracks would move poleward with large increases of intensity suggesting an increase of high impact storm events. Thus, the results of this study suggest that the Montreal Protocol possibly avoided strong NH climate changes.

1. Introduction

The 1987 Montreal Protocol on Substances that Deplete the Ozone Layer limited the worldwide production of ozone-depleting substances (ODSs). This agreement provided a mechanism for reducing and phasing-out the use of chlorofluorocarbons, halons, and other man-made ODSs.

An important step towards recognizing the Protocol's success is to investigate what might have happened to ozone and climate without a ban of ODS production. In an early study, *Prather et al.* [1996] simulated the impact of unrestrained CFC growth on stratospheric ozone by the year 2000 using a two–dimensional chemistry transport model. More recently, *Velders et al.* [2007] investigated the radiative forcing effect of uncontrolled increases of ODSs, which are also strong greenhouse gases (GHG). They found that in a so-called "World Avoided" (WA) scenario, with a 3% to 7% annual growth of ODS emissions, the radiative forcing by ODSs could have nearly matched that of anthropogenic CO_2 in 2010. The study by *Velders et al.* [2007] motivated more in depth climate studies of the WA scenarios by *Morgenstern et al.* [2008] and *Newman et al.* [2008] based on experiments with coupled Chemistry Climate Models (CCMs).

Newman et al. [2008] utilized the Goddard Earth Observing System chemistry-climate model (GEOS-CCM) version 1 [*Pawson et al,* 2008]. They carried out a transient WA simulation from 1974 to 2065 with an annual increase of ODS by 3%, one of the scenarios from *Velders et al*. [2007]. *Newman et al.* [2008] showed that 17% of the globally averaged column ozone is destroyed by 2020, and 67% is destroyed by 2065 with subsequent effects on stratospheric temperature and circulation.

Using the UK Chemistry and Aerosols (UKCA) climate-chemistry model in a time slice mode, *Morgenstern et al.* [2008] determined the climate response between two simulations that are forced with total chlorine loading of 3.5 ppbv (values of late 1990's) and 9 ppbv (equivalent to our "Word Avoided" in approximately 2020). Both simulations use Atmospheric Model Intercomparison Project 2 (AMIP2) sea surface temperatures (SST) and sea ice for the period 1989 to 1999 as lower boundary forcing. *Morgenstern et al.* [2008] found warming over the Arctic and North America, and cooling over Eurasia during winter, consistent with changes in the Northern Hemisphere Annular Mode (NAM). They also linked the warming near the Antarctic Peninsula during spring to a shift of the Southern Hemisphere Annular Mode (SAM) towards its positive phase.

In a companion study to *Newman et al*. [2008], we analyze GEOS-CCM simulations in more detail to determine the NH climate impact of severe stratospheric ozone depletions during the first half of the 21st century (C21). We will relate the results to sensitivity experiments that simulate stratospheric ozone recovery consistent with the successful ratification of international treaties [*WMO/UNEP*, 2003].

2. Model experiments

Table 1 summarizes the five GEOS-CCM simulations utilized in this study, comprised of a WA-simulation (#1) and four reference simulations (#2 to #5). We investigate three simulations that cover both the late 20th century (C20) and the first half of the 21st century (C20C21), and two simulations that cover the whole 21st century (C21). All simulations use observed GHG changes for the C20 and the Intergovernmental Panel on Climate Change (IPCC) GHG scenario A1b for C21. They also use prescribed SSTs as lower boundary forcings from IPCC scenario A1b ocean simulations as indicated in Table 1. *Eyring et al.* [2006] showed that past NH polar ozone changes simulated with the GEOS-CCM agree with observations. In the reference simulations, halogen forcing is based on observations and the Ab scenario [*WMO/UNEP*, 2003] for C20 and C21, respectively. The WA simulation (WA-CSST), forced with the 3% annual ODS increase, uses CCSM2 SSTs from 1974 to 2049.

Figure 1 illustrates the polar cap (66^{o}N-90^{o}N average) April total ozone. In the WA simulation, polar cap April total ozone decreases from 482 DU to 174 DU between 1974 and 2049 (Fig. 1). The 2001 to 2049 change is about 330 DU nearly twice the value observed from 1979 to 2000 in the Antarctic ozone hole [*Pawson et al.* 2008]. The runs C20C21-HSST and C20C21-CSST cover the period 1971 to 2049. The simulations show ozone decreases until 2000 of about 50 DU, stabilization at lower values until about 2010, and an increase to pre-ozone hole values up to 2049 (Fig.1). C21-CSST and C21-HSST both exhibit a general increase of Arctic total ozone.

3. Results

This study focuses on NH climate change during the first half of the 21st century, when the ozone changes in the WA-CSST simulation and the ensemble of the four reference simulations (C21-Rec) differ in sign (Fig. 1). Changes are investigated between the temporal means of the two 15 year periods 2001 to 2015 and 2035 to 2049. By comparing between changes for the WA-CSST and C21-Rec, the possible climate impacts of the Montreal Protocol can be determined.

Large changes of the annual cycle of stratospheric climate are observed in the WA-CSST experiment. Figures 2a-c show polar cap (66^o to 90^{o}N) ozone mixing ratio and temperature, and mid-latitude (50^{o}N-70^{o}N) zonal mean zonal wind. To address the significance of the NH stratospheric response, we compare the changes at stratospheric key levels between the WA-CSST and the ensemble mean C21-Rec (Figs. 2d-f) where the WA changes are largest in Figs. 2a-c. The 95% confidence intervals (red dashed lines in Figs. 2d-f) for the ensemble mean (solid red) are estimated using a t-test based on the standard deviation of changes in the four individual reference runs.

In the lower Arctic stratosphere, ozone decreases due to the increase of ODSs (Fig. 2a). Maximum ozone depletion of more than 2 ppmv can be found from January to April. These changes (e.g. at the 50 hPa level) significantly differ both in sign and magnitude form the ozone changes simulated in the C21-Rec ensemble (Fig. 2d). The ozone decreases in the troposphere (Fig. 2a) result solely from advection of depleted stratospheric ozone because the GEOS-CCM relaxes to a tropospheric ozone climatology below the tropopause. The lower stratospheric temperature cools (Fig. 2b) as a radiative response to the ozone depletion. Maximum cooling of 6K is found at the 100 hPa level during April and May. Fig. 2e reveals that the C21-Rec ensemble does not show any significant temperature change and the cooling simulated in WA-CSST experiment is outside of the C21-Rec confidence interval for all months except January. The polar cooling increases the meridional temperature gradient in the lower stratosphere and causes westerly wind anomalies (Fig. 2c). At the 50-hPa level anomalies larger 2 m/s are found from February - July and October - November. Values larger than 5 m s^{-1} are found in April consistent with the pronounced lower stratosphere cooling. Zonal wind changes during December - March are not statistically significant (Fig. 2f).

In general, the simulated NH polar stratospheric WA changes are consistent with observed [*Thompson and Solomon*, 2002] and simulated SH changes due to ozone depletion [e.g. *Perlwitz et al*. 2008]. Modeling studies showed that SH polar ozone losses have a strong impact on SH tropospheric circulation leading to a shift in the summertime SAM towards its positive phase [e.g., *Gillett and Thompson*, 2003; *Perlwitz et al.* 2008]. Several mechanisms have been proposed by which stratospheric climate changes could induce dynamical changes in the troposphere. They include direct radiative response [*Grise et al.*, 2008], downward control response [*Thompson et al.,* 2006], and a subsequent change in tropospheric eddies [e.g. *Song and Robinson,* 2004] or a direct response of tropospheric eddies to changes in stratospheric flow [*Chen and Held,* 2007].

Next, we investigate the impact of severe stratospheric polar ozone depletion on the NH troposphere. Fig. 3a shows overlapping 3-month averages of 500 hPa zonal mean zonal wind, where the label indicates the center month of the 3-month overlapping period. During winter, zonal wind decreases are found between 30^{o}N and 70^{o}N. During the other three seasons, the structure of the changes is different, with zonal wind increases between 50°N and 70°N and zonal wind decreases between 30°N and 50°N. This pattern is closely related to the NAM [*Thompson and Wallace*, 2000]. In Fig, 3b, we compare the changes in the NAM index. The pattern of the NAM was determined as the leading Empirical Orthogonal Function of the surface pressure field using the monthly fields of the C20C21-HSST simulation between 1971 and 2000. Clearly, the shift of the NAM index towards its positive phase in the WA scenario is significant during the late spring to fall season. During winter, the change in the NAM index is near zero and lies within the 95% confidence interval of the C21-Rec simulations. Thus, our results do not confirm *Morgenstern et al.* [2008], who suggested a decrease of the NAM index during winter in their WA simulation, while changes during other seasons were not discussed.

Figure 3c illustrates the temporal development of the standardized NAM index averaged for April to November. We show the time series of 15-year running mean values both for the WA-CSST and the C21-Rec ensemble where the labeling indicates the center year of a 15-year period. During this period, the NAM index time series of the C21-Rec ensemble exhibits a slight decrease to a value of about -0.2. Meanwhile, the index for WA-CSST hardly changes until about 2030, and then rapidly increases to 0.6 exceeding the confidence interval of the reference ensemble by about 2020.

Figure 4 compares the impact of this circulation change on lower troposphere temperature (left panels, Fig. 4) and upper air storm track activity (right panels, Fig. 4) for April to November averages. The latter is determined as the standard deviation of the 2.5-6 day band pass filtered 500-hPa geopotential heights [*Blackmon*, 1980]. Figure 4a shows the 925 hPa temperature changes in the C21-Rec simulation, which exhibits the known picture of tropospheric warming due to the GHG increase. The spatial pattern has a pronounced zonally symmetric structure with maximum warming of more than 2 K over polar latitudes. In the WA-CSST simulation (Fig. 4b), the warming over NH continents is enhanced (at least by 0.5 K) and most pronounced at sub-polar latitudes (1 - 1.5 K) and over Southern Europe (1 K). The difference pattern (Fig. 4c), which resembles the "world avoided", is consistent with the NAM-like circulation changes caused by horizontal temperature advection [*Thompson and Wallace*, 2000].

The April to November climatology (2001-2015) of 500hPa storm track activity (indicated by black solid lines in Fig. 4d and 4e) exhibits two main centers, one over the north Atlantic and one over the north Pacific. In the C21-Rec simulations (Fig. 4d), changes are small and show slight eastward expansion of the North Atlantic storm track and weakening of the north Pacific storm track. In the WA-CSST simulation (Fig.4e and 4f), a pronounced northward shift and enhancement of storm track activity can be found together with an eastward extension of the North Atlantic storm track. These features are consistent with the shift of the NAM towards its positive phase (Fig. 3c).

4. Discussion

Climate simulations based on CCMs can be used to quantify the outcome of international treaties that limited production of ODSs. In our study, we focused on the possible impact of a 3% per year increase of ODS production on the NH climate during the first half of the C21.

While the ratification of the Montreal Protocol has an important benefit for human health by avoiding extreme surface ultraviolet radiation [*Newman et al.* 2008], we also showed that it avoided very strong tropospheric circulation changes. We found that severe stratospheric ozone depletion in the NH polar stratosphere would have triggered stratospheric temperature and circulation changes that would cause a shift of the NAM towards its positive phase during late spring, summer, and fall. Subsequent implications for NH continental temperature and storm track activity are such that GHG induced warming over the NH continents would be amplified by up 100% and storm track activity would move poleward and strongly intensify. These changes are similar in structure to changes due to ozone depletion observed in the SH during the last three decades.

This study also illustrates that the climate impacts of the Montreal Protocol have to be seen in the light of increasing anthropogenic GHG concentration. Clearly our experiments suggest possible benefits of the Montreal Protocol by avoiding both temperature increases over the NH continents and extra-tropical storm events with possible high societal impacts. However, we also illustrated the pronounced warming over the Arctic as well as continental temperature increase due to GHG increase.

In the WA experiment, we prescribed SST and sea ice changes that are consistent with GHG increases of an IPCC scenario A1B. However, this lower boundary forcing does not take into account the radiative impact on SST that is caused by the increase of ODSs and the reduction of stratospheric ozone, both of which are also greenhouse gases. *Newman et al.* [2008] pointed out that SSTs used in the WA experiment are too cold compared with what would develop for the same scenario using a coupled atmosphere ocean model. Thus, a model configuration in which the CCM is coupled to an ocean/sea ice model is necessary to also consider the effect on ocean and sea ice changes and determine the full response of the climate system. Nonetheless, our results clearly illustrate the direct effects of stratospheric temperature and circulation changes of a WA scenario on the troposphere. For a more complete assessment of the Montreal Protocol accomplishments, various ODS scenarios should be investigated and simulations with other CCMs should be carried out.

Acknowledgments. This work was supported by the NASA Modeling and Analysis Program and used high-end computational resources provided by NASA's Columbia Project. R. Fogt's contribution was supported by the National Research Council Research Associateship Programs. We thank Martin Hoerling and William Neff for helpful discussion.

References

Blackmon, M. L., and N. C. Lao (1980), Regional characteristics of the Northern Hemisphere wintertime circulation: A comparison of the simulation of the GFDL general circulation model with observations, *J. Atmos. Sci.*, *37*, 497–514.

Chen, G., and I. M. Held (2007), Phase speed spectra and the recent poleward shift of Southern Hemisphere surface westerlies, *Geophys. Res. Lett.*, *34*, L21805, doi:10.1029/2007GL031200.

Eyring, V., et al. (2006), Assessment of temperature, trace species, and ozone in chemistry-climate model simulations of the recent past, *J. Geophys. Res.*, *111*, D22308, doi:10.1029/2006JD007327.

Grise, K.M., D. W. J. Thompson, and P.M. Forster (2008), On the Role of Radiative Processes in Stratosphere-Troposphere Coupling, *J. Clim.*, submitted.

Gillett, N., and D. W. J. Thompson (2003), Simulation of recent Southern Hemisphere climate change, *Science*, *302*, 273–275.

Morgenstern, O., P. Braesicke, M. M. Hurwitz, F. M. O'Connor, A. C. Bushell, C. E. Johnson, and J. A. Pyle (2008), The World Avoided by the Montreal Protocol, *Geophys. Res. Lett.*, *35*, L16811, doi:10.1029/2008GL034590.

Newman, P.A. et al. (2008), What would have happened to the ozone layer if chlorofluorocarbons (CFCs) had not been regulated? *Atmos. Chem. Phys. Discussion*, in review.

Pawson S., R. S. Stolarski, A. R. Douglass, P. A. Newman, J. E. Nielsen, S. M. Frith, and M. L. Gupta (2008), Goddard Earth Observing System chemistry-climate model simulations of stratospheric ozone-temperature coupling between 1950 and 2005, *J. Geophys. Res., 113*, D12103, doi:10.1029/2007JD009511.

Perlwitz, J., S. Pawson, R. L. Fogt, J. E. Nielsen, and W. D. Neff (2008), Impact of stratospheric ozone hole recovery on Antarctic climate, *Geophys. Res. Lett.*, *35*, L08714, doi:10.1029/2008GL033317.

Prather, M., P. Midgley, F. S. Rowland, and R. Stolarski (1996), The ozone layer: The road not taken, *Nature, 381*, 551–554.

Song, Y., and W. A. Robinson (2004), Dynamical mechanisms for stratospheric influences on the troposphere, *J. Atmos. Sci.*, *61,* 1711-1725.

Thompson, D.W.J., J.C. Furtado, and T.G. Shepherd (2006), On the Tropospheric Response to Anomalous Stratospheric Wave Drag and Radiative Heating, *J. Atmos. Sci.*, *63*, 2616-2629.

Thompson, D.W.J. and J.M. Wallace (2000), Annular modes in the extratropical circulation. Part I: Month-to-month variability, *J. Clim.*, *13*, 1000-1016.

Velders G. J. M., S. O. Andersen, J. S. Daniel, D. W. Fahey, and M. McFarland (2007), The importance of the Montreal Protocol in protecting climate, *Proc. Natl. Acad. Sci. U. S. A., 104*(12), 4814–4819, 10.1073/pnas.0610328104.

World Meteorological Organization (WMO)/United Nations Environment Programme (UNEP) (2003), Scientific Assessment of Ozone Depletion: 2002, World Meteorological Organization, Global Ozone Research and Monitoring Project, Report No. 47, Geneva, Switzerland.

Table 1 Time Period, SST Data set, Scenarios for Halogens and GHG for GEOS CCM Experiments

Number	Experiment	Period	SST	Halogens	GHG
1	WA-CSST	1974 - 2049	CCSM2	+ 3% /year	Observed/A1b
2	C20C21-HSST	1971 - 2049	HadGEM	Observed/WMO Ab	Observed/A1b
3	C20C21-CSST	1971 - 2049	CCSM2	Observed/WMO Ab	Observed/ A1b
4	C21-HSST	1996 - 2099	HadGEM	WMO Ab	A1b
5	C21-CSST	2001 - 2099	CCSM3	WMO Ab	A1b

Figure Captions:

Figure 1: Time series of NH polar cap (66^{o}N - 90^{o}N) total column ozone in April for experiments shown in Table 1. Thick lines show 11-year running mean.

Figure 2: *Top:* Monthly changes (2035-2049 minus 2001-2015) in (a) polar cap ozone (66^{o}N - 90^{o}N), (b) polar cap temperature (66^{o}N - 90^{o}N), (c) mid-latitude zonal wind (50^{o}N - 70^{o}N) for experiment WA-CSST. *Bottom:* Monthly changes (2035-2049 minus 2001-2015) at specific levels for WA-CSST (black) and C21-Rec (red) for d) 50 hPa polar cap ozone (66^{o}N - 90^{o}N), (e) 100 hPa polar cap temperature, and f) 50 hPa mid-latitude zonal wind. The dashed lines in panels d, e, and f indicate 95% confidence level for the C21-Rec simulations.

Figure 3: (a) 3-month overlapping changes (2035-2049 minus 2001-2015) in NH 500 hPa zonal mean zonal wind in [m s^{-1}]. (b) 3-month overlapping changes of standardized NAM index. (c) The 15-year running mean time series of April to November mean NAM index. In (b) and (c) black lines indicates the WA-CSST run, red lines indicates C21-Rec, and the dashed lines indicate the 95% confidence level.

Figure 4: *Left:* April to November changes (2035-2049 minus 2001-2015) of 925hPa temperatures [K]. *Top:* C21Rec, *middle:* WA-CSST and *bottom*: WA-CSST minus C21Rec. *Right*: Same as the left panels but for standard deviation of bandpass filtered (2.5-6 days) 500 hPa geopotential heights [m]. Solid lines in 4d and 4e indicate climatology determined from 2001-2015 mean. Shading in 4c and 4f indicate statistical significance at least at the 95% confidence level.

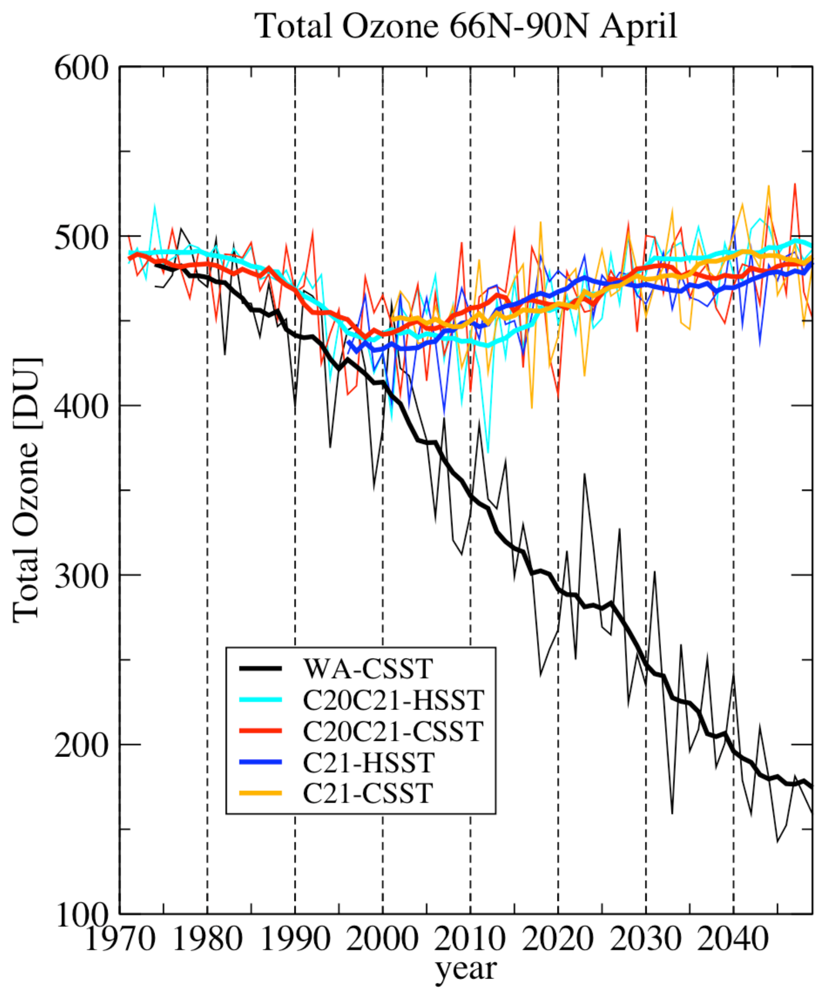
Total Ozone 66N-90N April
Total Ozone [DU]
600
500
400
300
200
100
1970
1980
1990
2000
2010
2020
2030
2040
year
WA-CSST
C20C21-HSST
C20C21-CSST
C21-HSST
C21-CSST

Figure 1:

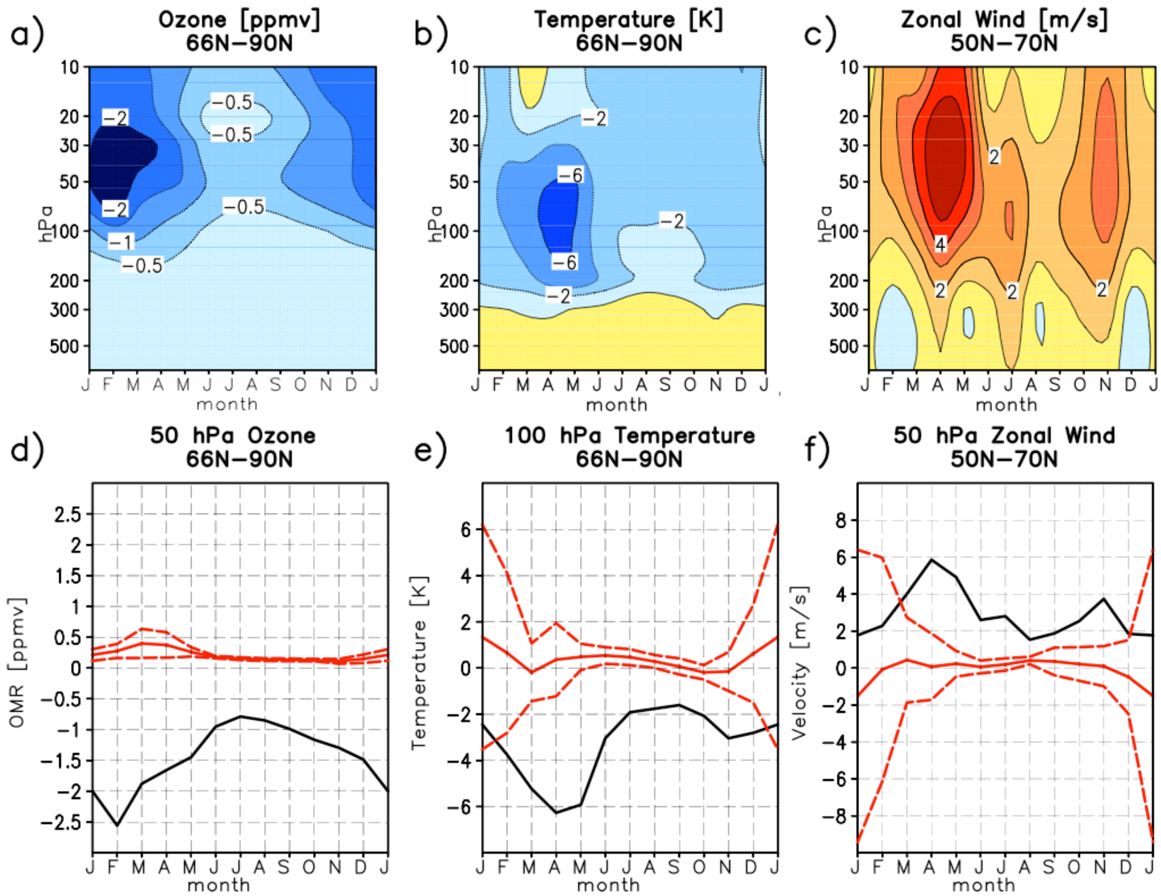
a) Ozone [ppmv] 66N–90N
b) Temperature [K] 66N–90N
c) Zonal Wind [m/s] 50N–70N
d) 50 hPa Ozone 66N–90N
e) 100 hPa Temperature 66N–90N
f) 50 hPa Zonal Wind 50N–70N
hPa
month
OMR [ppmv]
Temperature [K]
Velocity [m/s]
J F M A M J J A S O N D J

Figure 2:

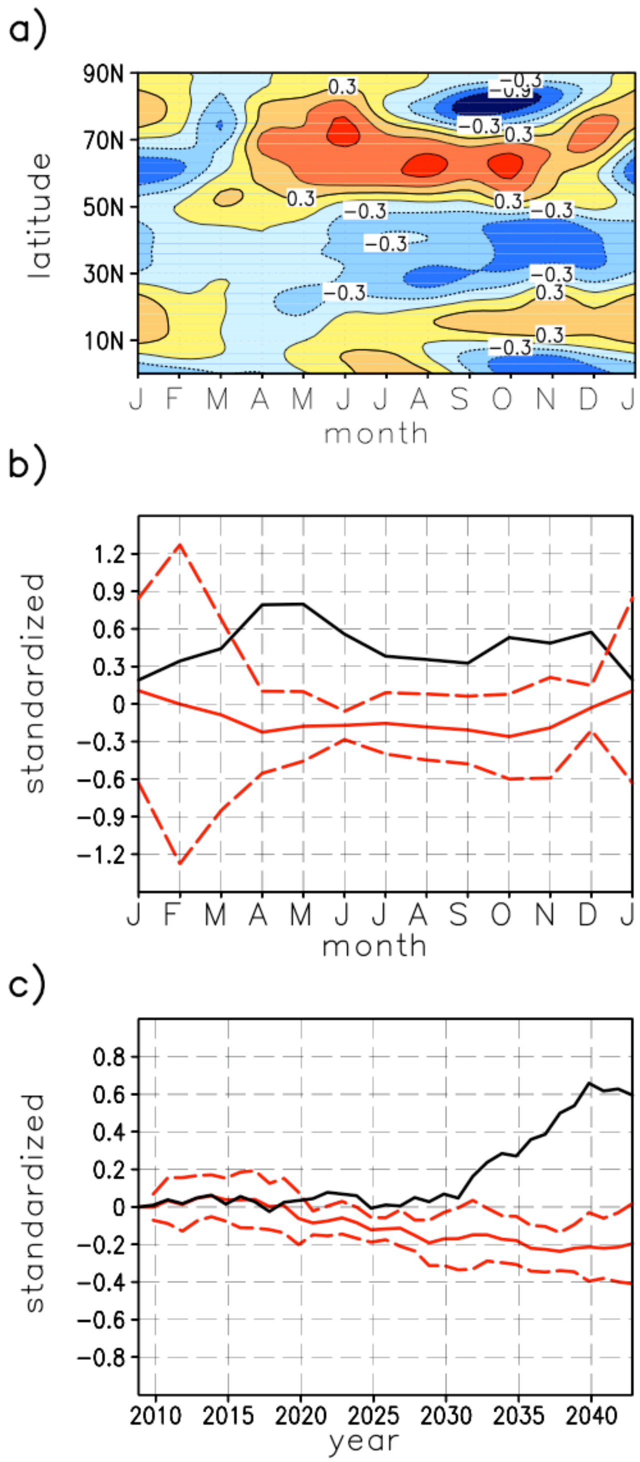
a)
90N
70N
50N
30N
10N
latitude
J F M A M J J A S O N D J
month
b)
1.2
0.9
0.6
0.3
0
−0.3
−0.6
−0.9
−1.2
standardized
J F M A M J J A S O N D J
month
c)
0.8
0.6
0.4
0.2
0
−0.2
−0.4
−0.6
−0.8
standardized
2010 2015 2020 2025 2030 2035 2040
year

Figure 3:

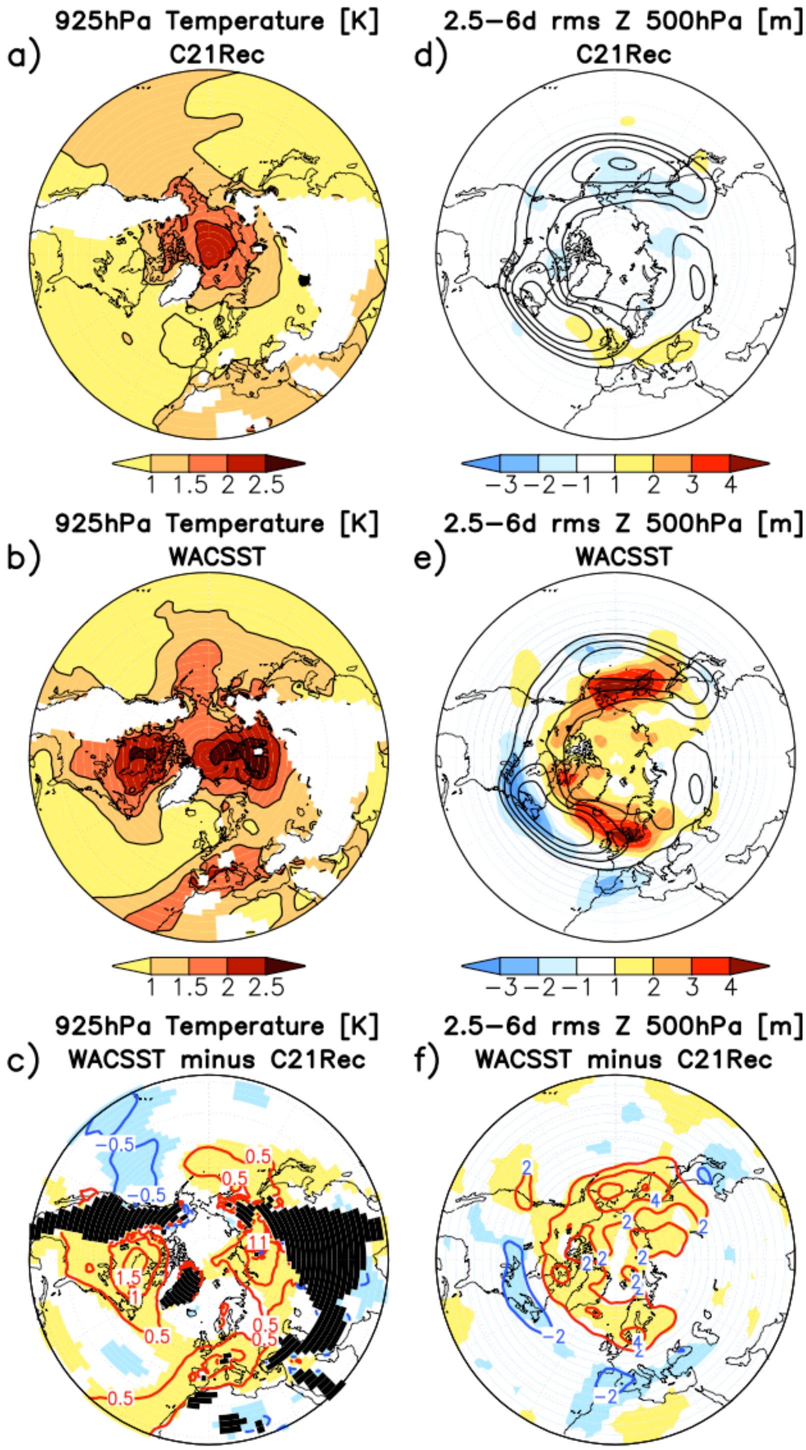
a)
925hPa Temperature [K]
C21Rec
1 1.5 2 2.5
d)
2.5–6d rms Z 500hPa [m]
C21Rec
−3 −2 −1 1 2 3 4
b)
925hPa Temperature [K]
WACSST
1 1.5 2 2.5
e)
2.5–6d rms Z 500hPa [m]
WACSST
−3 −2 −1 1 2 3 4
c)
925hPa Temperature [K]
WACSST minus C21Rec
f)
2.5–6d rms Z 500hPa [m]
WACSST minus C21Rec

Figure 4.